INVESTIGATING THE PERFORMANCE OF SAR POLARIMETRIC FEATURES IN LAND-COVER CLASSIFICATION

Liang Gao & Yifang Ban

Division of Geoinformatics, Royal Institute of Technology (KTH)
Drottning Kristinas väg 30, 10044 Stockholm, Sweden
mailto: - {liangg, yifang}@infra.kth.se

Youth Forum

KEY WORDS: SAR, Polarization, Multi-frequency, Land-Cover, Classification.

ABSTRACT:

This paper represents a study on land-cover classification using different polarimetric SAR features. The experiment is carried out using C- and L-band fully polarimetric EMISAR data acquired on July 5 and 6, 1995 over an agricultural area in Fjärdhundra, near Uppsala, Sweden. The polarimetric features investigated are coherency matrix, intensity of both *C*- and *L*-band SAR, and Cloud decomposition product *H(1-A)* of *L*-band, and 'entropy' texture of *L*-band *HV* intensity image. In order to investigate the performance of the different features, each feature is classified using a classifier that is best suited for the feature based on previous research. *H*/*A*/ α Wishart unsupervised classification is used for coherency matrix while neural network is applied to six "mean" texture layers of C and L bands fully polarimetric intensity images. The best classification accuracy was achieved using the intensity images combined with *H(1-A)* and 'entropy' texture (overall: 81%; kappa: 0.7). The producer's accuracy of intensity classification result for forest is 100.0% which reveals that the *H(1-A*) of *L*-band is a very good indicator for forest. The 'entropy' texture of *L*-band *HV* intensity image has the potential to be a good indicator for road with 77.2% user accuracy, while road is not discriminated in coherency matrix. The results indicate that the supervised classification of the intensity of both *C*- and *L*- bands has a good potential for land-cover mapping in this study area.

1. INTRODUCTION

Synthetic Aperture Radar (SAR) has been proven to be a powerful earth observation tool. The emerging Polarimetric SAR (POLSAR) adds another dimension to SAR information content, thus makes SAR remote sensing more applicable. Polarimetric SAR has been used in retrieval of soil moisture and surface roughness, snow and ice mapping and land-cover classification (Martini, 2004; Wakabayashi, 2004; T.Macri, 2003; J.Shi, 1997). Due to its sensitivity to vegetation, its orientations and various land-covers, SAR polarimetry has the potential to become a principle mean for crop and land-cover classification.

Many features such as intensities, coherency matrix, correlation and phase differences have been used in various classification experiments (Dorr, 2003; Hoekman, 2000; Lee & Grunes, 1994; Skriver, 2005; Alberga, 2007). As the information in the fully polarimetric data can not be completely represented by one single feature, the combination of different polarimetric features according to physical grounds and practical experiences should be considered. Most studies have focused on the specific methodology and specific polarimetric feature, few aims at systematically comparing the polarimetric features (Alberga, 2007). Thus, research is needed to evaluate different polarimetric features in a systematic manner.

The objective of this research is to evaluate the performance of fully polarimetric multi-frequency SAR features in land-cover classification. The investigation is carried out by classification of the polarimetric features and comparing the classification results. Coherency matrix, intensity, Cloud decomposition product *H(1-A)*of *L*-band, and 'entropy' texture of *L*-band *HV* intensity image will be evaluated and compared.

2. POLARIMETRIC FEATURES

The polarimetric features investigated in this study are reviewed in the following sections.

COVARIANCE MATRIX

The polarimetric SAR measures the amplitude and phase of backscattered signals in four combinations of the linear receive and transmit polarizations: *HH*, *HV*, *VH* and *VV* (H for horizontal and V for vertical polarization, respectively).
EMISAR data have two available polarimetric features:

1). Scattering matrix data *S* in slant range projection.

2). Covariance matrix data *C* in pseudo ground range.

Since the SAR data is stained by speckles, the speckles can be filtered at the expense of loss of spatial resolution with multi-look processing. In this case, a more appropriate representation of *S* is the covariance matrix in which the average properties of a group of resolution cells can be expressed in a single matrix (Allan, 2007). It is defined as (van Zyl and Ulaby, 1990b):

$$< C >= \begin{bmatrix} < S_{hh}S_{hh}^{*} > & < S_{hh}S_{hv}^{*} > & < S_{hh}S_{vv}^{*} > \\ < S_{hv}S_{hh}^{*} > & < S_{hv}S_{hv}^{*} > & < S_{hv}S_{vv}^{*} > \\ < S_{vv}S_{hh}^{*} > & < S_{vv}S_{hv}^{*} > & < S_{vv}S_{vv}^{*} > \end{bmatrix} \quad (1)$$

where S_{ij} is scattering matrix, * denotes the complex conjugation. This covariance matrix C follows a complex Wishart distribution (Lee and Grunes, 1994).

INTENSITY

The diagonal elements of $< C >$ can be linear transformed to the intensities of HH, HV and VV polarizations respectively (Hoekman, 2007). In this study, the three real matrices were used as input of the intensity feature. Since it is already multi-looked, the speckle is supposed to be reduced to a certain extent.

COHERENCY MATRIX

Coherency matrix can be linear transformed from covariance matrix as follows (Lee, 1999):

$$< T >= N < C > N^T \qquad (2)$$

where $$N = \frac{1}{\sqrt{2}} \begin{bmatrix} 1 & 0 & 1 \\ 1 & 0 & -1 \\ 0 & \sqrt{2} & 0 \end{bmatrix}$$

The coherency matrix representation has the advantage over the covariance matrix of relating to underlying physical scattering mechanisms. In order to get meaningful entropy in Entropy/ α decomposition, the coherency matrix should be multi-look processed or speckle filtered (Lee & Grunes, 1999). In this study, filtered single-look coherency matrix was used as input.

H(1-A)

Entropy/ α decomposition proposed by Cloude and Pottier (1997), is often used recently in polarimetric classification researches (T.Macri, 2003; Lee & Grunes, 1999; Coulde and Pottier, 1997). *H*, and α represent the decomposition parameters generated after the calculation of coherency matrix's eigenvalues. This method provides a way to partition the polarimetric feature space in a logical way, where *H* stands for entropy arises as a natural measure of the inherent reversibility of the scattering data and α identifies the underlying average scattering mechanism. In other word, the entropy describes the purity of the scattering components and α describes the type of the scattering mechanism. *A* is an additional parameter sometimes added into the decomposition, standing for anisotropy; it provides further information on the number of scattering components.

It is reported that with *L* band, *H* and *A* can be used to discriminate forest from more deterministic media (Martini, 2005). In this study, we use $H(1-A)$ as a forest indicator. The specific $H(1-A)$ term is equal to 0 in case of deterministic scattering and reaches 1 when the scattered wave polarization is random.

3. EXPERIMENTS

3.1 Study Area and Data Description

The study area is an agricultural area in Fjärdhundra, near Uppsala, in Sweden. The major land-cover types are agriculture (further divided into six crop types), road, forest, and clear cut. The classification schemes for each classification are list below. Due to confusion among several classes in the C- and L-band coherency matrix, classifications of these coherency matrices did not include some classes:

1) Intensity of both *C* and *L* bands: 'Road', 'Forest', 'Clear Cut', 'Crop1'-'Crop6'.

2) L-band coherency matrix: 'Forest', 'Clear Cut', 'Crop1'-'Crop3', 'Crop5', and 'Crop6';

3) C-band coherency matrix: 'Forest', 'Crop1'- 'Crop6';

The experiment SAR data were acquired by Danish fully polarimetric EMISAR with dual-frequency (*C*- and *L*- band) over the study area on July 5 and 6, 1995. This is part of the European Multi-sensor Airborne Campaign: EMAC-95. The nominal resolution of single-look image is 2m x 2m. The covariance matrix after processing has a resolution of 5m x 5m. Figures 1-2 show the Pauli composition images for *C* and *L* bands.

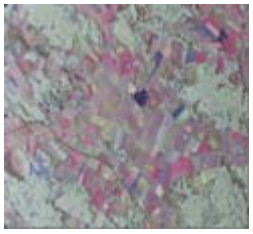

Figure 1. C-band image

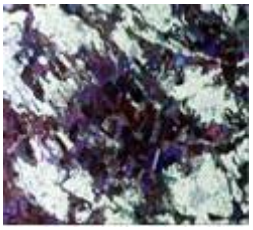

Figure 2. L-band image

3.2 Classification

Since the characteristics of different polarimetric features differ from one another, the classifier which is proven to be effective for each polarimetric feature based on previous studies was chosen to achieve the best performance for each feature. In this study, two different classification methods were carried out.

3.2.1 Wishart Unsupervised Classification

H/*A*/ α Wishart unsupervised classification method (Lee & Grunes, 1999) was based on the polarimetric decomposition developed by Cloude and Pottier (Coulde and Pottier, 1997). This method exploits the coherent information in fully polarimetric SAR data and is an effective automated

classification method. In this study, the method is applied separately on the single-look coherency matrices of both *C* and *L* bands EMISAR data. The following processes were performed during the classification:

Single-look coherency matrix is filtered by 7x7 refined Lee filter.

(1) Calculating of engenvalues, so-called $H/A/\alpha$ polarimetric decomposition.
(2) Finally, the data is classified by complex Wishart classifier.

3.2.2 Neura Network Classification

Hara (1994) found that neural network is a good method for polarimetric SAR classification and therefore the method is chosen for classification of the intensity of *HH*, *HV* and *VV* of both *C* and *L* bands polarimetry SAR data.

To evaluate the polarimetric feature 'intensity', we use the multi-looked (2 looks) intensity layers of *HH*, *HV* and *VV* of both *C*- and *L*- bands. Although the data have been filtered by multi-look processing, the speckle still retained. Thus, we performed texture analysis prior to classification. Based on our previous experience on the classification of the same area, the 'mean' texture is useful for classification. While the 'entropy' texture is good for discriminate the homogeneous targets from deterministic areas, it introduces the noise into other areas. Based on the above considerations, a classification method was developed as below:

- Generate 'mean' and 'entropy' texture from six intensity layers.
- Generate forest mask, using the product of polarimetric decomposition. Set the pixel of which $H(1-A)>0.7$ as forest.
- Generate masks for road and crop6 using the classification result by applying neural network on 'entropy' texture of L-band HV intensity layer.
- Mask out the data using the masks generated above.
- Select training area for the remaining land-cover types.
- Applied neural network classifier on the masked six 'mean' texture layers

Overall accuracy (OA), kappa coefficient together with producer's accuracy (PA) and user's accuracy (UA) are used as accuracy measurement.

4. EXPERIMENTAL RESULTS

The experimental results are discussed following the manner of the polarimetric features investigated and their performances on the land-cover classifications are evaluated.

Figures 3-5 are the classification maps for both classification methods. Table 1 shows PA, UA, overall accuracy and Kappa coefficient for all the classification results.

$H(1-A)$

As described earlier, $H(1-A)$ of *L*-band SAR was used as an indicator of forest. We tested a series of thresholds from 0.60 to 0.75. 0.65 is suggested in Martini (2005) for summer forest, but we found 0.7 was better for our study area, as more clear cut areas were not being masked. This can be observed from Figure 6-8. All the masks were filtered by 9x9 median filter.

Class	L-Band Coherency Matrix		C-Band Coherency Matrix		C-, L- band Intensity	
	PA %	UA %	PA %	UA %	PA %	UA %
Forest	76.50	72.10	60.70	63.90	100.00	92.00
Road	N/A		N/A		71.70	77.20
Crop6	93.00	78.80	99.00	78.60	94.00	61.80
ClearC	55.00	85.90	N/A		74.00	92.50
Crop1	65.00	47.40	73.00	70.90	76.00	100.00
Crop2	44.00	69.80	80.80	80.80	77.00	62.60
Crop3	39.00	45.30	68.10	70.10	85.00	77.30
Crop4	N/A		67.70	62.00	52.00	67.50
Crop5	56.00	50.70	51.50	51.70	99.00	78.60
OA	62.30		66.30		81.00	
Kappa	0.576		0.622		0.700	

Table 1. Accuracy Assessment

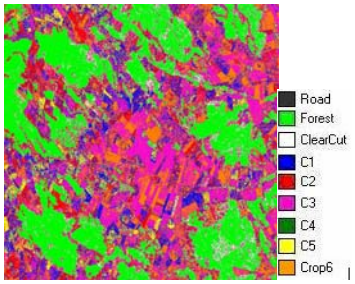

Figure 3. L-band Coherency matrix Classification Result

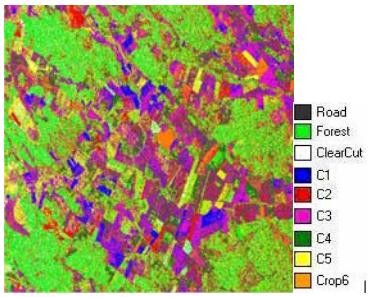

Figure 4. C-band Coherency matrix Classification Result

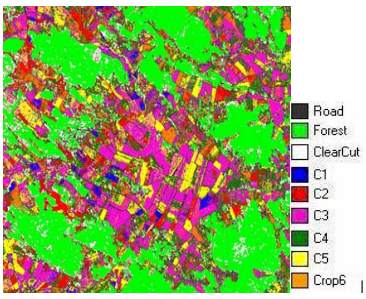

Figure 5. C, L bands Intensity Classification Result

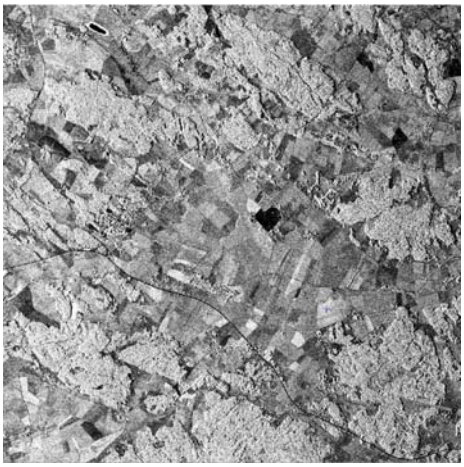

Figure 6. C-band HH image

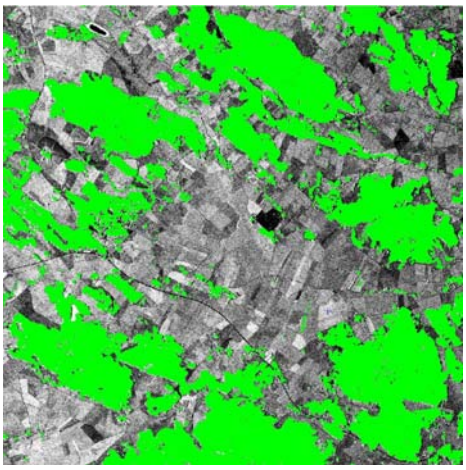

Figure 7. Forest Mask with threshold 0.65

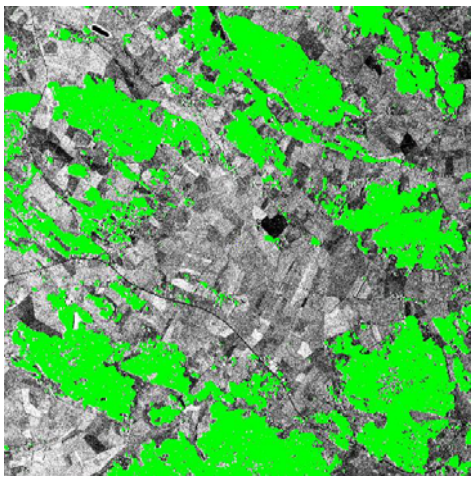

Figure 8. Forest Mask with threshold 0.7

From the accuracy assessment, the *C* and *L* bands intensity classification in which the forest mask was used has the highest accuracy for 'Forest', which is 100% in PA, 92% in UA. The result is much better than using the whole coherency matrix of which the best PA accuracy is only 76.5%. $H(1-A)$ is indeed a good indicator for forest. And the threshold we used is suitable for this study.

The bigger the threshold is, the less the forest is recognized. Further experiment is needed to figure out whether it can also be used to classify the forest according to the forest volume, and what is the threshold. However it should be pointed out that roads in the forest is mixed with forest in both mask images.

INTENSITY

Combining with other polarimetric features: $H(1-A)$ and "entropy" texture of *L*-band *HV* intensity image, the overall accuracy of the intensity classification is better than that of the single-look coherency matrix. The OA is 81%, and Kappa achieved 0.70. It also recognized the most land-cover types. Part of the reason is that we use three masks in the classification for the intensity and the data were filtered two times: multi-look and texture analysis. The accuracies for the crops are good. PA is around 80% for four crop types. 'Crop5' was best classified with the PA 99.0%. But 'Crop4' has a relative low accuracy, with the PA 52% only.

The accuracy of the 'entropy' texture of *HV* polarization of *L* band intensity image achieved PA 71.70% for 'Road' and 94.00% for 'Crop6'. Since 'Road' was not recognized in coherency matrix, this result was relative good. Although the coherency matrix has a higher accuracy for 'Crop6', it should be noted that this class is combined with other land-cover types as we described before.

COHERENCY MATRIX

In this study, the land-cover classification of coherency matrix is not as effective as that of intensity. Both C-band and L-band have a lower OA accuracy than intensity. However, C-band data is better than L-band data in crop classification.

The main reason for the low classification accuracy was the speckle level in the image. The speckle in the image decreased the classification accuracy. Higher accuracy was produced by using intensity because two filterings were performed, while in coherency matrix, only one filtering was carried out. More filtering will be tested in the further study, using, for example, MAP filter (H. Skriver, 2005).

5. CONCLUSION

This study evaluated the performance of different polarimetric features for land-cover classification in order to develop an effective classification procedure. Two polarimetric features: coherency matrix and intensity were investigated by classification of the whole image. Other two polarimetric indicators: $H(1-A)$ of L-band and "entropy" texture of *L*-band *HV* intensity image were evaluated as a classifier for one or two specific land-cover types.

The results indicate that the supervised classification of the intensity of both *C*- and *L*- bands has the potential for land-cover mapping in this study area. The results also revealed that both classification results of coherency matrix and the intensity can be improved. It is very difficult to find one polarimetric feature that will be effective for all land-cover types. A hierarchical classification approach is highly desirable. The second classification method in this study is a good attempt and the result is also promising. More polarimetric features need

to be evaluated following the similar manner to exploit the potential of fully polarimetric SAR data for land-cover classification.

ACKNOWLEDGEMENT

This research was support by a grant from the Swedish National Space Board awarded to Professor Ban. The authors thank the European Space Agency for providing the EMISAR images. Liang Gao would like to thank the Swedish Cartographic Society for providing travel grant to ISPRS 2008 Congress.

REFERENCES

Allan A. Nielsen, Henning Skriver et al., 2007. Complex Wishart distribution based analysis of polarimetric synthetic aperture radar data, *Proceedings of MultiTemp 2007*.

DH. Hoekman, MJ. Quiriones, 2000. Land cover type and biomass classification using AirSAR data fore evaluation of monitoring scenarios, *IEEE Trans.on Geosci. Remote Sensing*, Vol. 38, Issue 2, pp.685-696.

Dirk H. Hoekman, Thanh Tran, and Martin Vissers, Unsupervised full-polarimetric segmentation for evaluation of backscatter mechanisms of agricultural crops, *POINSAR 2007*,http://earth.esa.int/workshops/polinsar2007/papers/71_hoekman.pdf (accessed 20 April. 2008)

Dorr. D. G., Walker. A., et al., 2003, Classification of urban SAR imagery using object oriented techniques, *IGARSS'03 Proceedings*, pp: 188-190.

E.L. Christensen and J. Dall, 2002. EMISAR: A dual-frequency, polarimetric airborne SAR, *IGARSS'02. 2002 IEEE International*. Vol.3, pp: 1711-1713..

Hara,Y., Atkins, R.G., et al., 1994. Application of neural networks to radar image classification, *IEEE Trans.on Geosci. Remote Sensing*, Vol. 32, Issue 1, pp. 100-109.

H. Skriver, J. Dall, et al., 2005. Agriculture classification using POLSAR data, *Proc. PolinSAR 2005*.

J.J. van Zyl and F.T.Ulaby, 1990. Scattering matrix representation for simple targets, in *Radar Polarimetry for Geoscience Applications*, F. T. Ulaby and C. Elachi, Eds. Artech, Norwood, MA.

Jong-Sen Lee and Grunes, M.R., et al., 1999 Unsupervised classification using polarimetric decomposition and the complex Wishart classifier, *IEEE Trans.on Geosci. Remote Sensing*, Vol.37, Issue5, pp: 2249-2258.

J.Shi, J.Wang, A.Y. Hsu, P.E.O'neill, and E.T.Engman, 1997. Estimation of bare surface soil moisture and surface roughness using L-band SAR image data, *IEEE Trans.on Geosci. Remote Sensing*, Vol. 35, pp.1254-1266.

J.S. Lee, M. R. Grunes, 1994. Classification of multi-look polarimetric SAR imagery based on complex Wishart distribution, *Int. J. Remote Sensing*, Vol. 15, No. 11, pp: 2299-2311.

Martini, A., ferro-famil, L., et al., 2005. Dry snow extent monitoring using multi-frequency and multi-temporal polarimetric indicators, *Radar Conference* 2005, pp: 173-176.

Martini.A., Ferro-Famil.L., Pottier.E., 2004. Multi-frequency polarimetric snow discrimination in Alpine areas, *IGARSS'04 Proceedings*, Vol.6, pp: 3684-3687.

S. R. Coulde and E. Pottier, 1997. "An entropy based classification scheme for land applications of polarimetric SAR":, *IEEE Trans.on Geosci. Remote Sensing*, Vol.35, pp: 68-78.

T.Macri Pellizzeri, 2003. Classification of polarimetric SAR images of suburban areas using joint annealed segmentation and "H/A/α" polarimetric decomposition, *ISPRS Journal of photogrammetry and remote sensing*, Vol. 58, Issues 1-2, pp: 55-70.

V.Alberga, 2007. A study of land cover classification using polarimetric SAR parameters, *Int. J. Remote Sensing*, Vol. 28, No. 17, pp. 3851-3870.

Wakabayashi.H., Matsuoka.T., Nakamura.K., Nishio.F., 2004. Polarimetric Characteristics of sea ice in the sea of Okhotsk observed by airborne L-band SAR, *IEEE Trans.on Geosci. Remote Sensing*, Vol. 42, Issue 11, pp: 2412-2425.